

Analysis of the effect of blade positions on the aerodynamic performances of wind turbine tower-blade system in halt states

Shitang Ke^{*1,2}, Wei Yu^{1a}, Tongguang Wang^{1b}, Yaojun Ge^{2c} and Yukio Tamura^{3d}

¹Department of Civil Engineering, Nanjing University of Aeronautics and Astronautics, Nanjing 210016, China

²State Key Laboratory for Disaster Reduction in Civil Engineering, Tongji University, Shanghai 200092, China

³Wind Engineering Research Center, Tokyo Polytechnic University, 1583 Iiyama, Atsugi, Kanagawa 243-0297, Japan

(Received April 23, 2016, Revised January 10, 2017, Accepted January 13, 2017)

Abstract. The unsteady flow field disturbance between the blades and tower is one of the primary factors affecting the aerodynamic performance of wind turbine. Based on the research object of a 3MW horizontal axis wind turbine which was developed independently by Nanjing University of Aeronautics and Astronautics, numerical simulation on the aerodynamic performance of wind turbine system in halt state with blades in different position was conducted using large eddy simulation (LES) method. Based on the 3D unsteady numerical simulation results in a total of eight conditions (determined by the relative position with the tower during the complete rotation process of the blade), the characteristics of wind pressure distributions of the wind turbine system and action mechanism of surrounding flow field were analysed. The effect of different position of blades on the aerodynamic performance of wind turbine in halt state as well as the disturbance effect was evaluated. Results of the study showed that the halt position of blades had significant effect on the wind pressure distribution of the wind turbine system as well as the characteristics of flow around. Relevant conclusions from this study provided reference for the wind-resistant design of large scale wind turbine system in different halt states.

Keywords: wind turbine system; halt state; blade position; large eddy simulation; aerodynamic performance; parameter analysis

1. Introduction

Horizontal axis wind turbine is one of the most efficient wind energy conversion device which consists primarily of high-rise tower and flexible blades, and it is a typical wind-sensitive structure (Karimirad and Moan 2011, Agarwal and Manuel 2009). The rotation of blades and flow around affect the surrounding flow field of the tower, resulting in the modification of the characteristics of intensively varied flow field in the local surrounding area of the tower. In particular, when the

*Corresponding author, Associate professor, E-mail: keshitang@163.com

^a Postgraduate, E-mail: yuweinuaa@163.com

^b Professor, E-mail: tgwang@nuaa.edu.cn

^c Professor, E-mail: yaojunge@tongji.edu.cn

^d Professor, E-mail: yukio@arch.t-kougei.ac.jp

wind turbine in halt state is subjected to high wind velocity, different blade position causes significant difference in the wind pressure distribution of the tower and blades themselves. It is therefore of great engineering significance to accurately predict the aerodynamic load of wind turbine in halt state.

The previous studies (Ke *et al.* 2015, Jeong *et al.* 2013, Guo *et al.* 2013, Corson *et al.* 2012, Greaves *et al.* 2012, Griffith *et al.* 2008, Larsen *et al.* 2007, Tempel 2006, Duquette and Visser 2003) on aerodynamic loads of large wind turbine system including tower and blades have two major problems: (1) No existing study was found on the qualitative and quantitative evaluation on the effect of different blade position during halt state on the wind loads of the wind turbine system. (2) The action mechanism of surrounding flow field and vorticity distribution of wind turbine tower-blade system in halt state as well as the disturbance effect was not revealed. Although the latest studies (Tran *et al.* 2015, Liu *et al.* 2015) revealed the aerodynamic characteristics and wind-induced vibration mechanism of the large wind turbine tower-blade system considering the aeroelastic effect, and also found that the FAST (fatigue, aerodynamic, structure, and turbulence) codes were changed considerably depending on the amplitude and frequency of the platform surge motion. However, the research of blade positions on the aerodynamic performance of wind turbine system in halt state is relatively less, especially on interference mechanism between tower and blade of large wind turbines.

With respect to the gap, a 3 MW horizontal axis wind turbine was selected as research object in this study. Based on LES method the numerical simulation on the aerodynamic performance of the wind turbine system in halt state with different blade position was conducted. The surface wind load and flow around characteristics of the wind turbine system in eight different cases of calculation (determined by the relative position between the full rotation process of the blade and the tower), the effect of different blade position on the aerodynamic performance and disturbance effect of wind turbine system in halt state was evaluated. Results from this study provide reference for the wind resisting design of large scale wind turbine in halt state.

2. Geometric model and calculating conditions

Taking a selected 3MW horizontal axis three-blade wind turbine as example, the detailed parameters are given as follows: the height of the tower was 85 m, the radius of the top of the tower was 2.0 m and the radius of the bottom of the tower was 2.5 m; the tower was linked variable-thickness structure with a thickness of the top wall of 30 mm and the bottom wall, 60 mm; the cut-in wind speed was 3.5 m/s, rated wind speed was 12.5 m/s, the cut-out wind speed was 25 m/s and the tilt angle of the wind turbine was 5° ; the angle between each blade was 120° and the blades were evenly distributed along the circumference; the length of the blade was 44.5 m and the detailed parameters of each blade element section along the wingspan are given in Table 1. The dimension of the engine room was $12\text{ m} \times 4\text{ m} \times 4\text{ m}$ (length \times width \times height). Components such as blades, engine room and wheel hub were established in sequence according to the above design parameters and the 3D tower-blade model of large scale wind turbine was built by Boolean calculation, as shown in Fig. 1.

According to the relative position of the blade and tower, with consideration of the periodicity during the rotation of three-blade system, a total of eight calculating conditions were setup with an initial state of 0° between the blade and vertical direction with an increment 15° of along clockwise direction. The specific positions are demonstrated in Fig. 2.

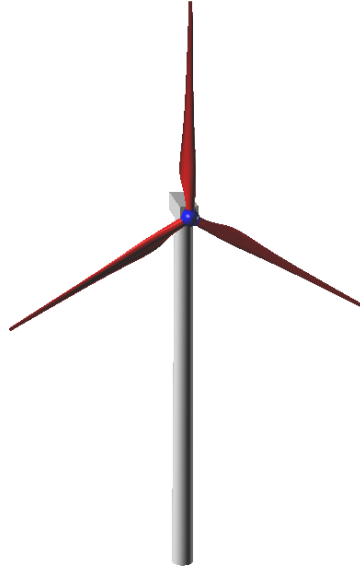


Fig. 1 Schematic diagram of the 3D model of a large scale wind turbine system

Table 1 Parameters of wind turbine blades

Position %	Radius r/m	Chord length C/m	Inflow angle $\varphi/^\circ$	Pitch angle of the blade element $\beta/^\circ$
5	2.225	2.561	0.823	37.140
10	4.450	4.646	0.640	26.672
15	6.675	4.389	0.507	19.069
20	8.900	3.808	0.414	13.692
25	11.125	3.228	0.346	9.830
30	13.350	2.738	0.296	6.976
35	15.575	2.313	0.258	4.802
40	17.800	1.970	0.229	3.103
45	20.025	1.686	0.205	1.742
50	22.250	1.448	0.186	0.630
55	24.475	1.246	0.169	-0.293
60	26.700	1.074	0.156	-1.072
65	28.925	0.925	0.144	-1.736
70	31.150	0.796	0.134	-2.310
75	33.375	0.682	0.125	-2.810
80	35.600	0.582	0.118	-3.250
85	37.825	0.492	0.111	-3.640
90	40.050	0.412	0.105	-3.987
95	42.275	0.340	0.099	-4.299
100	44.500	0.275	0.095	-4.580

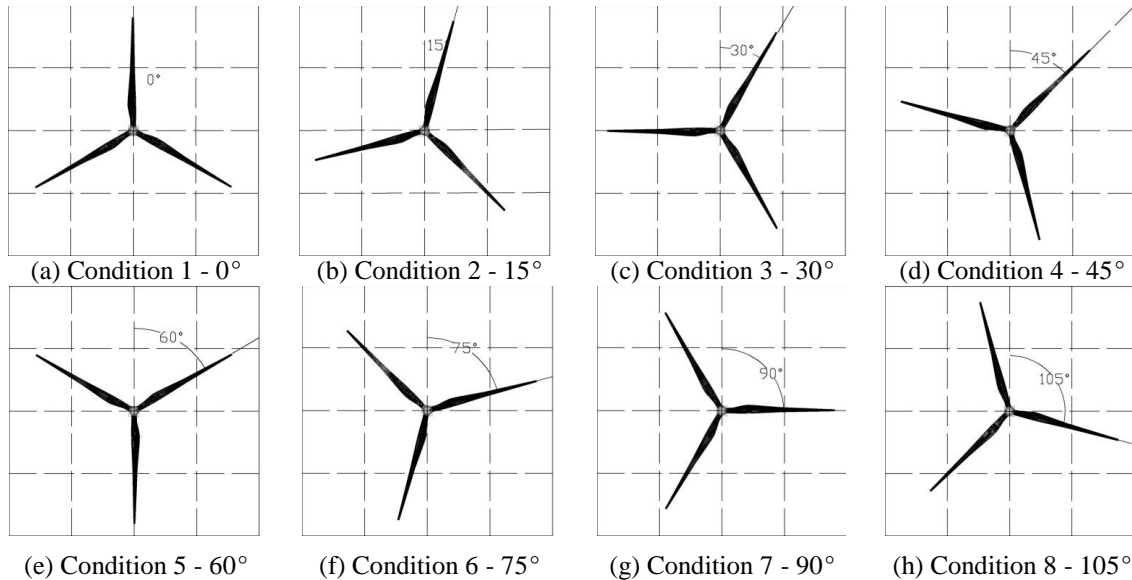


Fig. 2 Schematic diagram of calculating conditions

3. Parameter setup for numerical simulation

3.1 Calculating domain and meshing

In order to completely develop the flow field, the calculating domain was taken as $12D \times 5D \times 5D$ (flow direction $x \times$ span-wise direction \times vertical direction, D is the diameter of blade rotation). The wind turbine was setup at a distance of $3D$ to the entry of the calculating domain to ensure that the wake flow can fully develop in $8D$. Due to the complexity of the blade surface, hybrid mesh discrete mode was used and the complete calculating domain was divided into two parts, where the core region was meshed by tetrahedron and local mesh around the wind turbine was encrypted, while the outer region was meshed by fine hexahedron mesh. The total number of mesh was 7.95 million. The calculating domain and details of meshing are shown in Fig. 3.

3.2 Boundary conditions and turbulence model

The boundary condition of the entry was defined as velocity entry in which the ground roughness coefficient of the wind velocity section was 0.15 and the basic wind velocity at a reference height of 10 m was 25 m/s with respect to the cut-out velocity of the wind turbine. The distribution form with respect to type B geologic conditions in China was used for the turbulence strength section. The boundary condition of inflow and FLUENT were connected by user-defined function (as shown in Fig. 4). The boundary condition of the exit was defined as pressure exit with a relative pressure of 0. Non-slipping surface was used for the ground of the calculating domain and the surface of the wind turbine, and the side and symmetric boundary conditions were used for the top surfaces of the calculating domain.

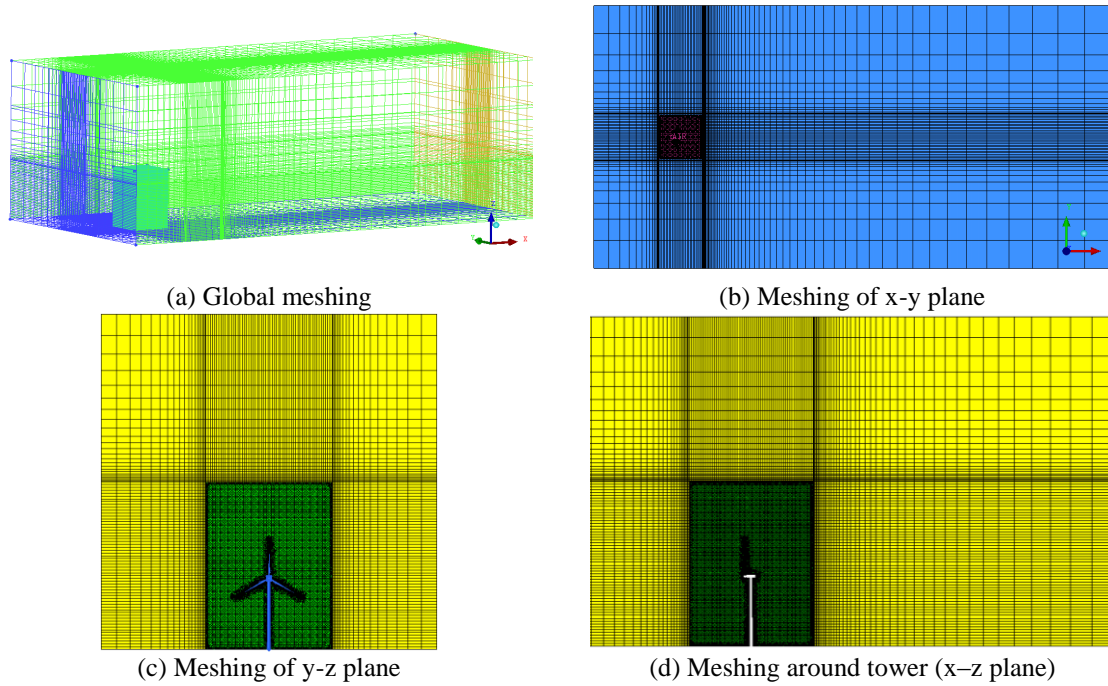


Fig. 3 Schematic diagram of the calculating domain and encrypted meshing

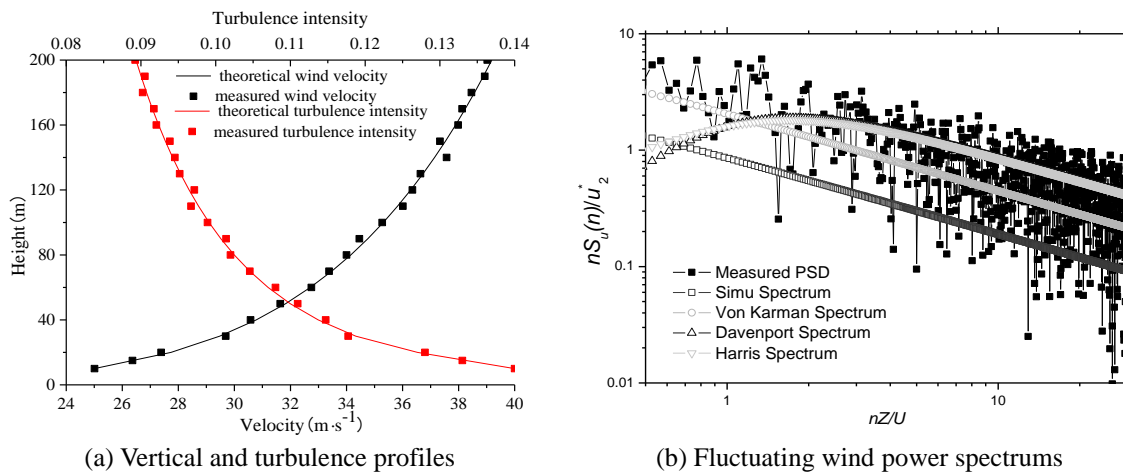


Fig. 4 Comparison of Simulation parameters between LES and the measured results

3D single precision discrete solver was used in numerical calculation. Due to the flow field where the wind turbine located was unsteady constant and the condition of turbulence flow was complex, the complicated flow field of wind turbine can be better simulated by LES (Hoogedoorn *et al.* 2010, Jiménez *et al.* 2010). Smagorinsky-Lilly model was used for sub-grid scale and the

pressure-velocity coupling equation sets were solved by SIMPLEX format which has good convergence and is suitable for LES calculation with small time step. Standard format was used for the discrete pressure item, Bounded Central Differencing format was used for dynamic discrete and second order implicit differential equation was used for transient equation. The residual difference of calculation of control equations was 1×10^{-6} which was calculated by the model height and the average wind velocity at the model height with a time step of 0.001s.

4. Analysis of aerodynamic performance

4.1 The validity checking

In order to verify the effectiveness of simulation method for wind turbine tower-blade system, Fig. 5 shows the distribution of average pressure coefficient and fluctuating wind pressure coefficient of the typical cross section at 30m height which was less affected by blades, and these compared with the standard (GB 50009-2012 2012) and the measured distribution curve (Li *et al.* 2015, Nishimura and Taniike 2001) both at home and abroad.

The results show that the distribution of average wind pressure coefficient by the large eddy simulation is almost same as given by standard, only the value on the leeward face are slightly less than standard value, which could be caused by the aerodynamic interference from blades. The fluctuating wind pressure distribution curve is among the measured curve at home and abroad, and the distribution trend with circumference is relatively close. However, taking into consideration that the fluctuating wind pressure distribution are closely related to the terrain of the measured tower, inflow turbulence and the surrounding disturbances, the fluctuating wind pressure distribution trend and values were obtained by LES both in the envelope of the measured results, the comparison demonstrates that the simulating method of aerodynamic performance for wind turbine system in this paper is accurate and steady.

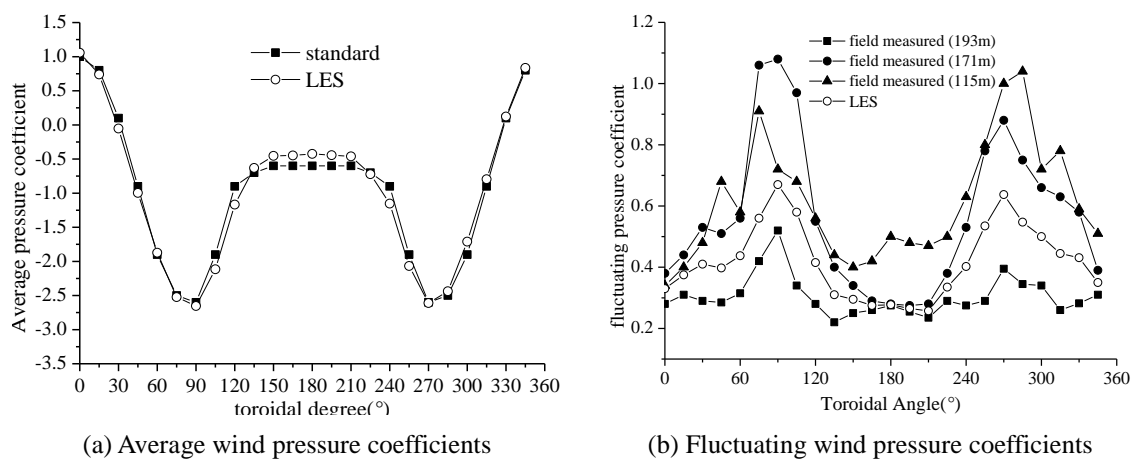


Fig. 5 Comparison of results between LES and the measured results

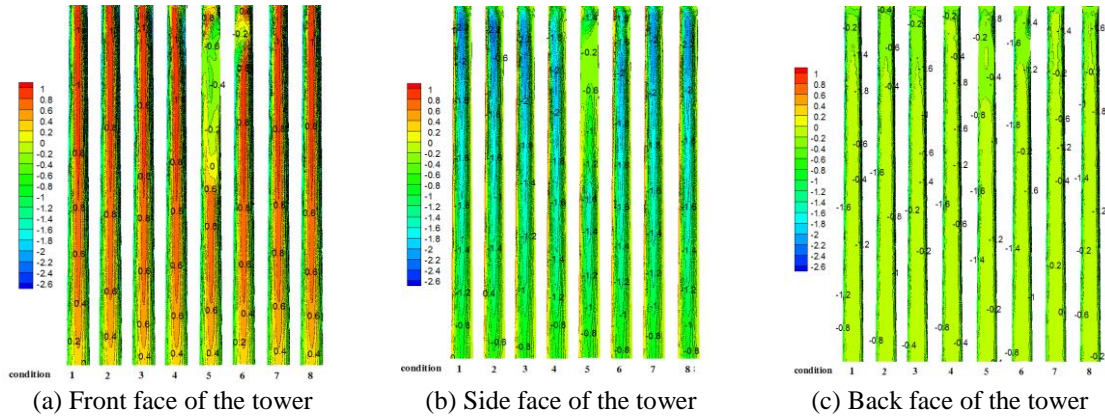


Fig. 6 Contour of pressure coefficient of the tower in different conditions

4.2 The static wind pressure

Fig. 6 shows the contour of pressure coefficients of the tower in eight conditions. It is evident that the narrow and long positive pressure distribution zone appeared on the windward face of the tower in the condition that the blades did not obstruct the tower, and the pressure increased with the increase in height. Negative pressure distribution appeared on side and leeward areas of the tower and the negative pressure at side areas were significantly larger than that on leeward areas. In the conditions where the blades in inflow direction obstructed the tower to different extends, negative pressure distribution zone appeared in the obstructed area on the windward area of the tower, and the negative pressure reduced with the increase of obstructed area. The disturbance of blades led to a reduction of negative pressure on side surfaces of the tower and different positions of blades had little effect on the leeward area of the tower.

Denote the blade with 0° angle to the vertical direction as Blade 1 and the other two blades were denoted as Blade 2 and Blade 3 in clockwise sequence. Fig. 7 shows the contour of the pressure coefficient of the three blades in different conditions. It is evident from Figure 7 that the windward faces of the blades in different conditions and in halt state were all positive pressure zones and the leeward face were negative pressure zone. Due to the blades of upwind wind turbine were not obstructed in the inflow direction, the distribution of positive pressure on the windward face of each blade in different conditions was similar and the pressure in the centre was larger than in the edges. The distribution of negative pressure at the leeward face was rather even and the distribution of pressure coefficient for Blades 1 and 3 was similar, where negative pressure with a value of -0.4 appeared on about $1/3$ of the span-wise direction and -0.8 appeared on the apex. On the other hand, the disturbance effect between Blade 2 and the tower was evident and distribution of negative pressure different from Blades 1 and 3 were witnessed. When the blade was located as in conditions 5 and 6, the distribution of negative pressure was about -0.6 and -0.4 respectively. The pressure coefficient at the apex was about -0.6 which was smaller than Blades 1 and 3.

Table 2 shows the global shape coefficient of the tower and each blade. It is evident that the global shape coefficient of the tower was significantly smaller than that of each blade, which indicates that the wind load is more sensitive to the complex shape of the blade than the tower with

circular cross-section. In addition, due to the obstructive effect of the blades on the tower, negative pressure distribution was found on the obstructed area on the windward face of the tower, and thus the global shape coefficient of the tower in conditions 5 exhibited significant trend of reduction. The variation of global shape coefficient for Blades 1 and 3 in each condition was similar, where the shape coefficient increased when the relative position of the blades and the tower was closer.

4.3 Fluctuating wind pressure coefficient

According to different relative position of the turbine and tower, Fig. 8 shows the time history diagram of pressure coefficient of the windward face of the tower at a height of 30 m and 70 m. It is evident from Fig. 7 that in the conditions when there was no obstruction to the tower by the blades, the pressure coefficient of the tower in the disturbed region was close to that in the undisturbed region. However, when the blades obstructed the tower to different extent, the pressure coefficient in the two regions varied significantly and the difference increased with the increase in the extent of obstruction.

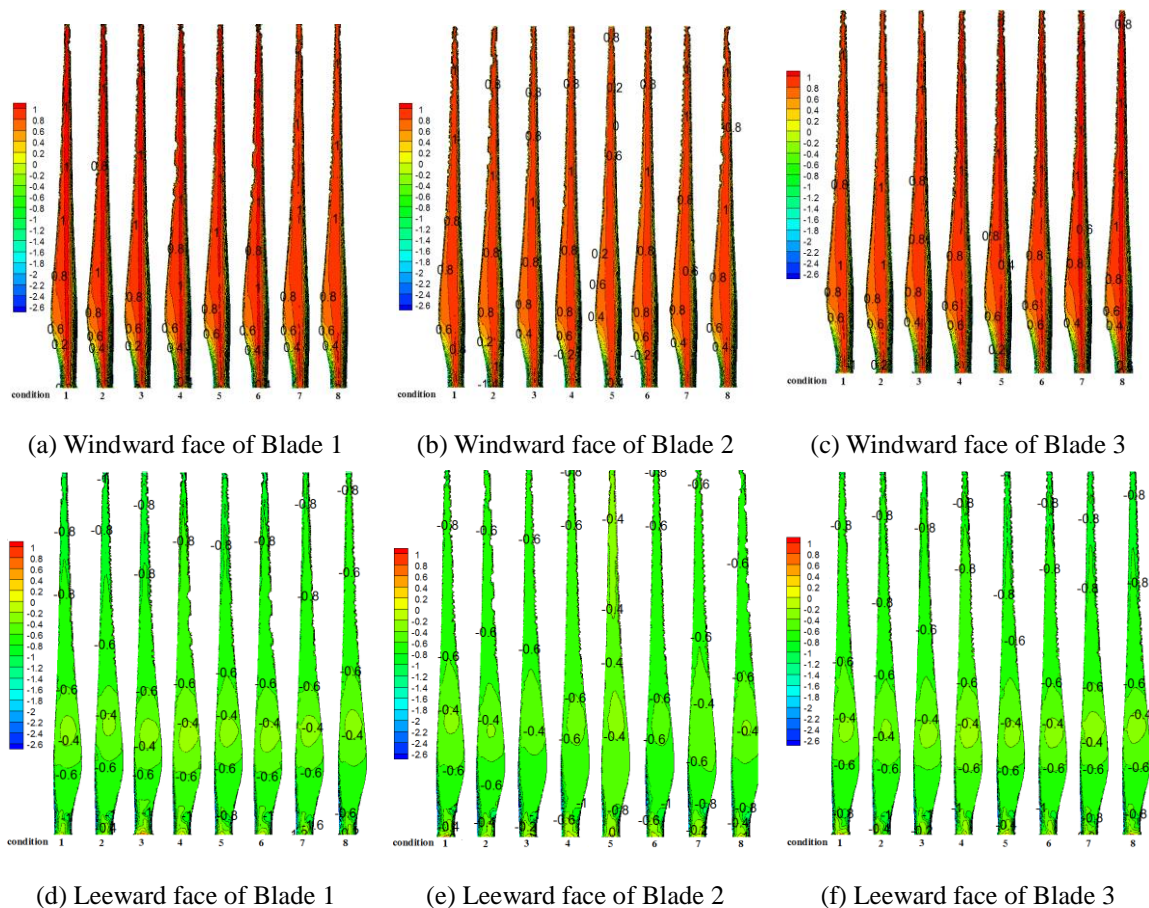


Fig. 7 Contour of the pressure coefficient of the blades in different conditions

Table 2 Global shape coefficient of the tower and each blade in different conditions

Position	Condition 1	Condition 2	Condition 3	Condition 4	Condition 5	Condition 6	Condition 7	Condition 8
Tower	0.522	0.524	0.524	0.436	0.271	0.549	0.478	0.507
Blade 1	1.752	1.767	1.730	1.750	1.802	1.823	1.804	1.808
Blade 2	1.778	1.847	1.872	1.927	1.617	1.861	1.850	1.836
Blade 3	1.816	1.801	1.825	1.804	1.790	1.789	1.749	1.767

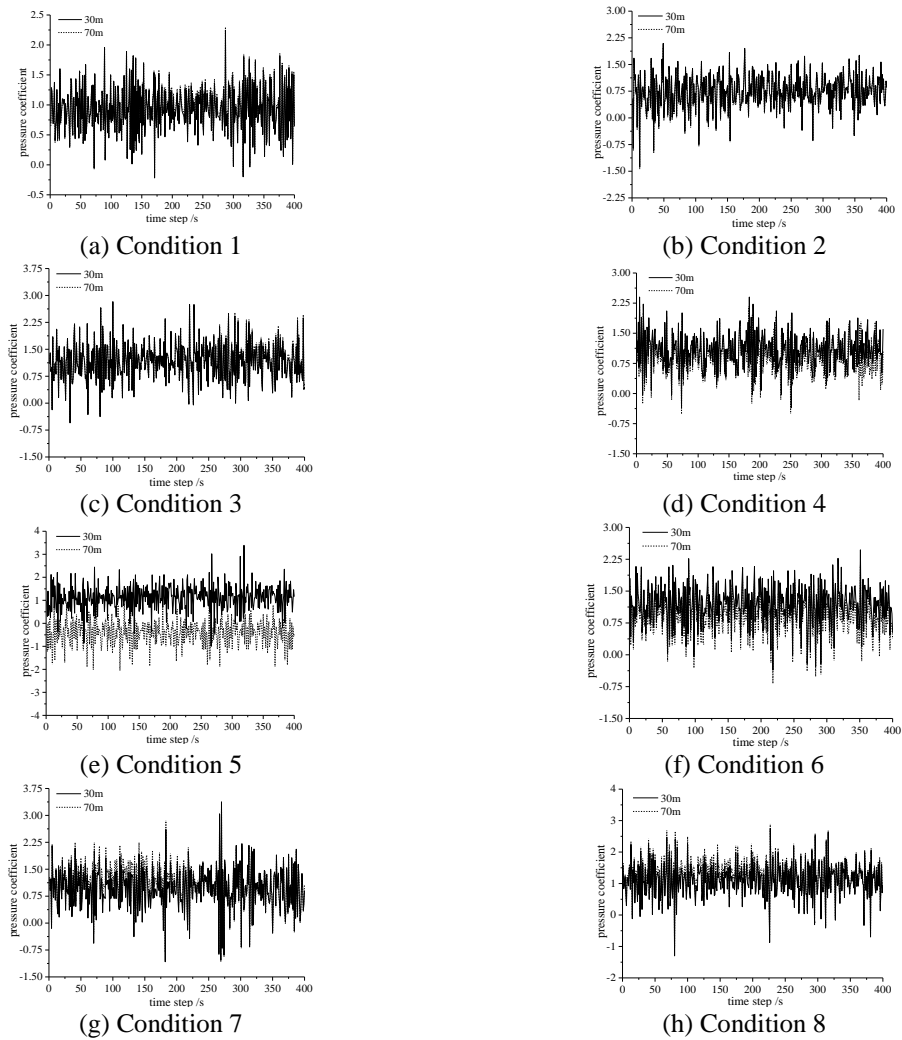


Fig. 8 Time history of pressure coefficient on the windward area for the tower in different conditions

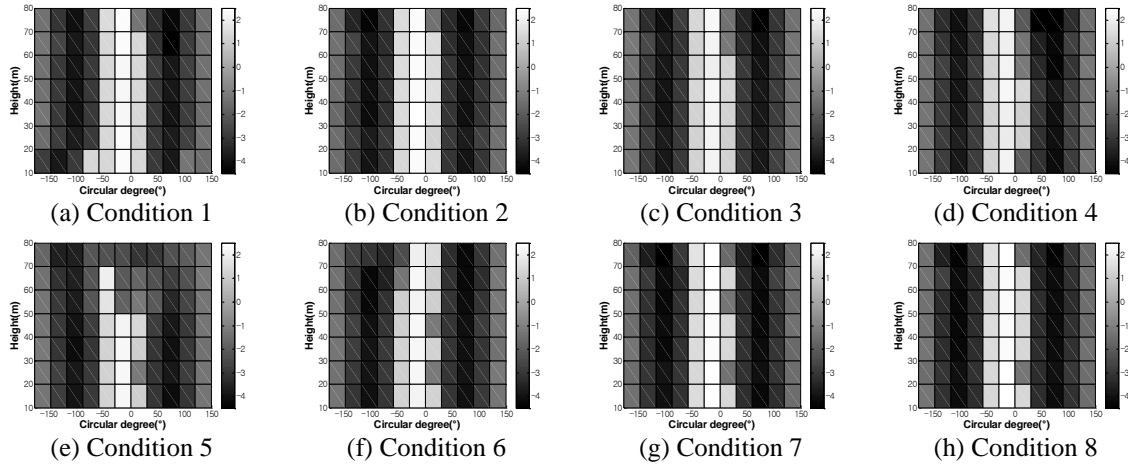


Fig. 9 The peak values of wind pressures coefficients of the tower in different conditions

Fig. 9 shows the peak value of wind pressure coefficients of tower in different conditions, with the peak value factor taken as 2.5. Results showed that different position of blades in halt state had significant effect on the peak wind pressure on different parts of tower. The maximum pressure coefficients of different conditions were appeared on the windward side position, as the relative position of the blades and the tower was closer, owing to the distribution of negative pressure in the parts of tower windward side which was obscured by blades, the maximum pressure coefficient was decreased. The minimum wind pressure was appeared on the tower side, and the values would be increased when the position was more close to the top of the tower. Meanwhile, the disturbance of blades led to a reduction of negative pressure on side surfaces of the tower, it was also caused the reduction of minimum wind pressure.

Table 3 shows the calculated peak wind pressure coefficient at typical measuring points of each components of the wind turbine system, with the peak value factor taken as 2.5. Results showed that different position of blades in halt state had significant effect on the peak wind pressure on different components of the wind turbine. It is recommended that the least favourable condition be considered during the wind resistance design of large scale wind turbine.

Table 3 Peak wind pressure coefficient at tip of blades of the wind turbine system

Location	Condition 1	Condition 2	Condition 3	Condition 4	Condition 5	Condition 6	Condition 7	Condition 8
Tip of blade1	2.227	2.179	2.089	1.980	2.022	1.996	2.255	2.303
Tip of blade2	2.231	2.033	1.891	1.903	1.713	2.153	2.284	1.947
Tip of blade3	2.221	2.339	2.110	1.972	2.164	2.079	2.288	2.220

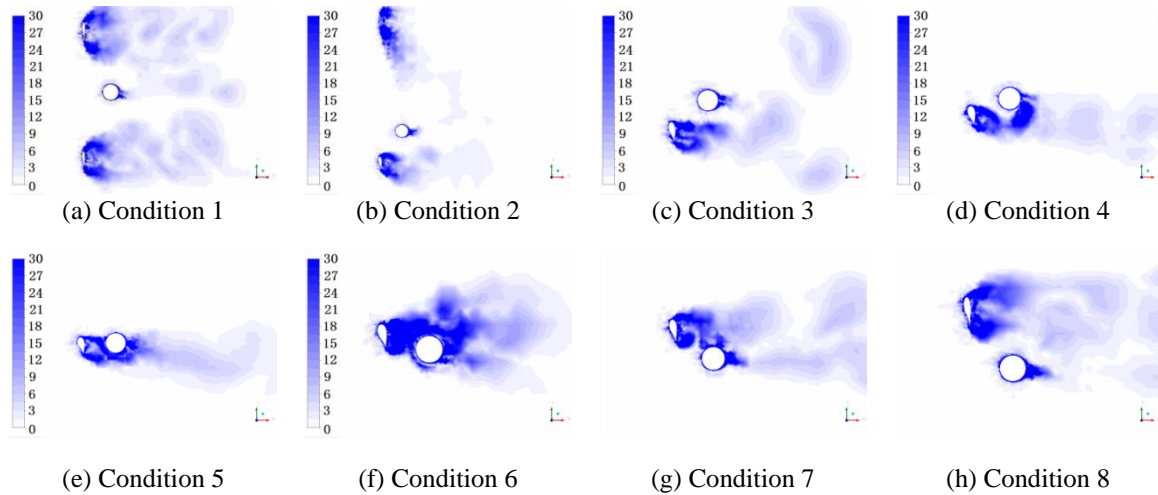


Fig. 10 Distribution of vorticity of blades and tower of the wind turbine system at the height with distinctive disturbance

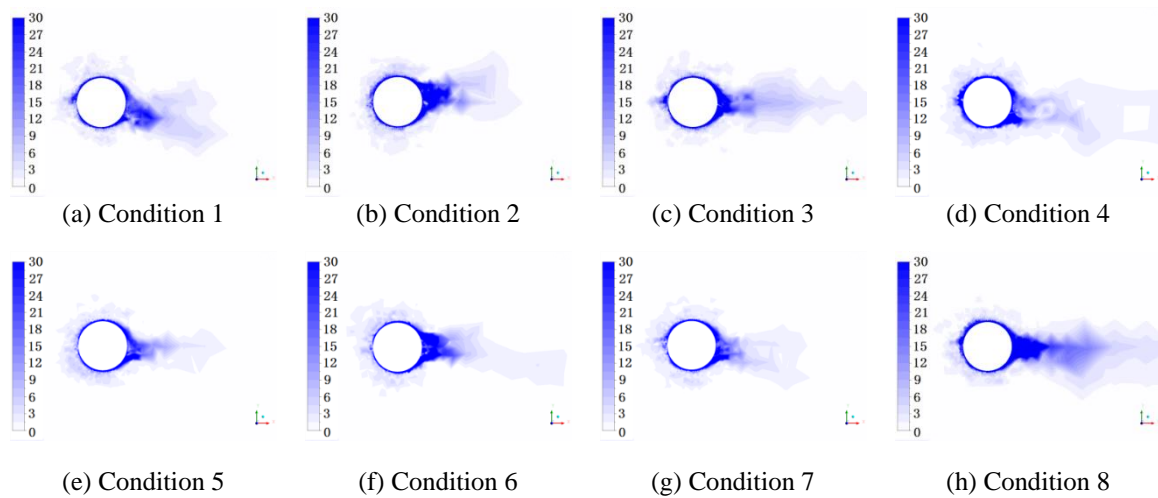


Fig. 11 Distribution of vorticity of blades and tower of the wind turbine system at the height with indistinctive disturbance

4.4 Characteristics of vorticity distribution

Figs. 10 and 11 respectively show the vorticity distribution of blades and tower of the wind turbine system at the heights with distinctive and indistinctive disturbance in different conditions. It is evident that obvious vorticity increment region appeared on the leeward face of the tower and blades. With the rotation of the blade position, the wake vortex region at the back of the tower was more obvious when the relative position of blades and tower was closer. The range of vorticity induced by the root of the blades was significantly larger than the wake vortex region of the tower.

In Conditions 3 and 7, large vorticity increment region was found in the location with no obvious blade section, i.e., evident apex vortex appeared.

Judging from the rotation position of the three blades, only the rotation of Blade 2 passed through the tower, so Fig. 12 shows the vorticity distribution of Blade 2 in different conditions. It is clear that: (1) inflow attached to the surface of the engine room and vortex appeared at the back of the engine room in each condition, which was the primary cause of negative pressure distribution at the leeward face of the engine room. (2) The leeward face of the blade mainly consisted of attached flow and small scale attached vortex was formed on the surface of the blade. The vorticity distributed evenly long the span-wise direction. Also, obvious vorticity increment appeared at the location close to the blade root at the leeward face of the blade. (3) With the increase of degree of obstruction by the blades to the tower, the degree of blade-tower interaction increased and large scale vortex was formed at the back. (4) In condition 5, the blade provided obstructive on the inflow, vortex was formed at the tower centre by flow around the blade which attached to the flow around the tower and formed large scale vortex at the leeward face of the tower. (5) Obvious apex vortex and blade root vortex appeared at the wake flow field of the blades of the wind turbine, and trailing edge vortex of the blade occurred between the root and the apex of the blades.

4.5 Flow field analysis

Fig. 13 shows the velocity streamlines of typical sections of the wind turbine system. It was found that due to the obstruction of blades, flow separation of the inflow was witnessed and the separated flow attached to the surface of the blade. Part of the inflow became vortex at the leeward face of the blades when passed through the front and back edges of the blades, and small scale vortex was formed on the surface close to the blades. The flow and vortex shedding were the main reason that negative pressure was formed on the leeward face of the blade. When the distance between the tower and blades was close enough, the vortex moved between the leeward face of the blade and the windward face of the tower. As a result, the negative pressure appeared at the windward face of the tower in Conditions 5 and 6.

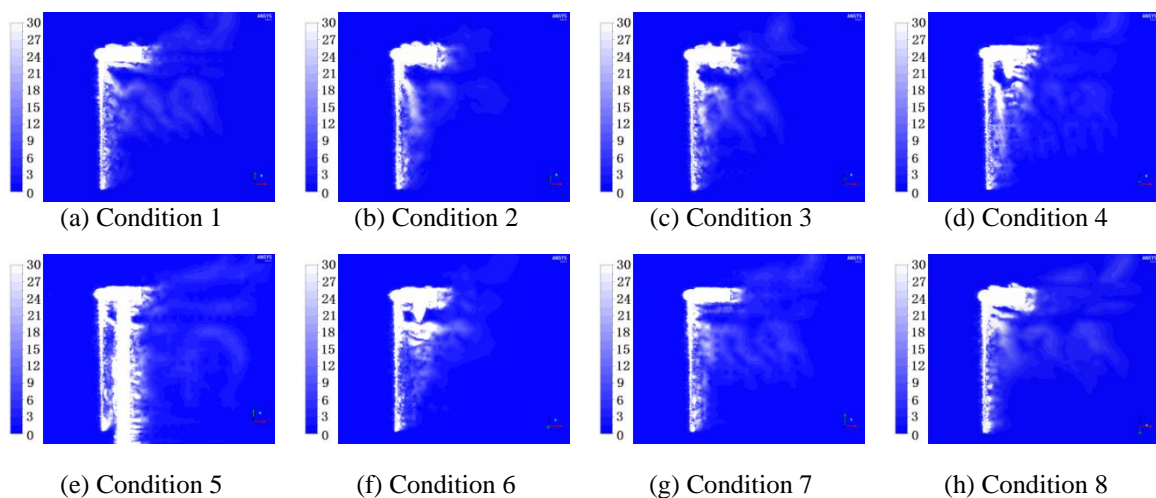


Fig. 12 Distribution of vorticity of blade 2 of the wind turbine system

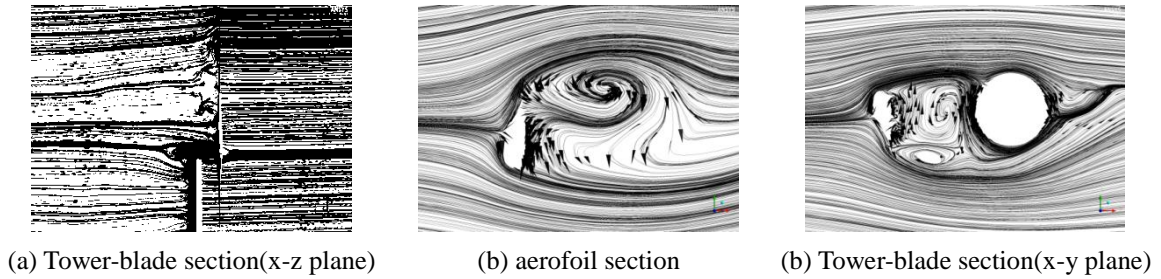


Fig. 13 Streamline of typical section of the wind turbine system

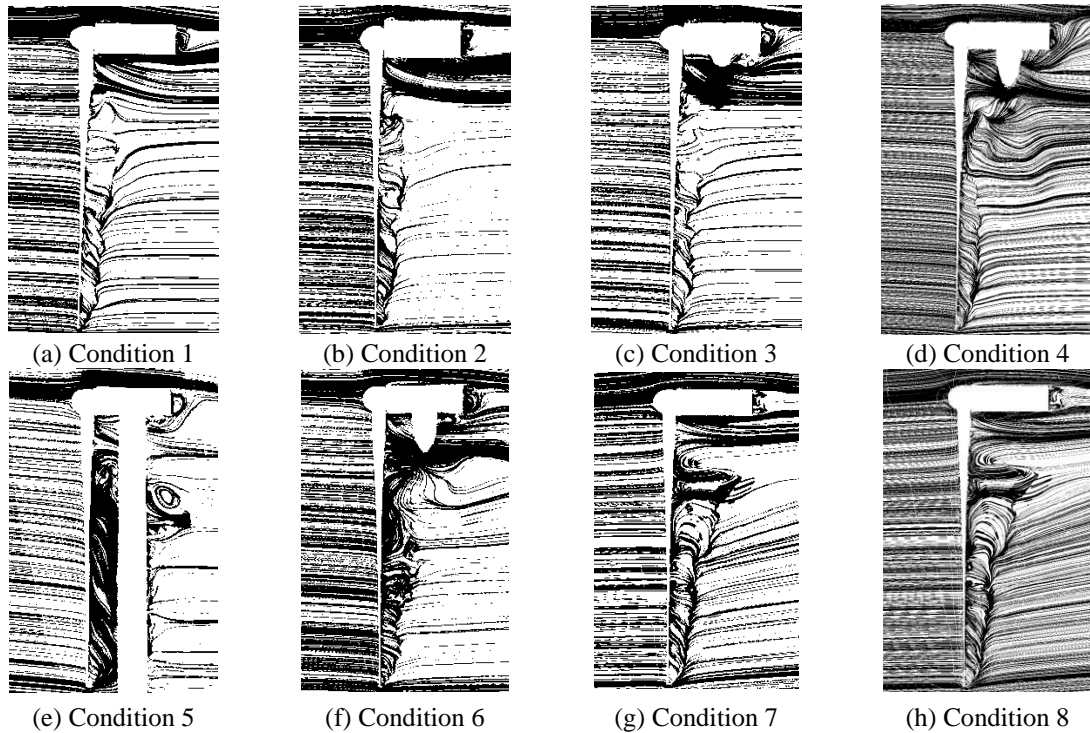


Fig. 14 Velocity contour and streamline of Blade 2 in different conditions

Fig. 14 shows the streamlines of Blade 2 at different rotating positions. The conclusions acquired from this figure are similar to that in Fig. 13. In addition, it can be seen from flows that obvious separated flow appeared at the location close to the blade root at the leeward face of the blade, and it is well explained the vorticity distribution in Fig. 13

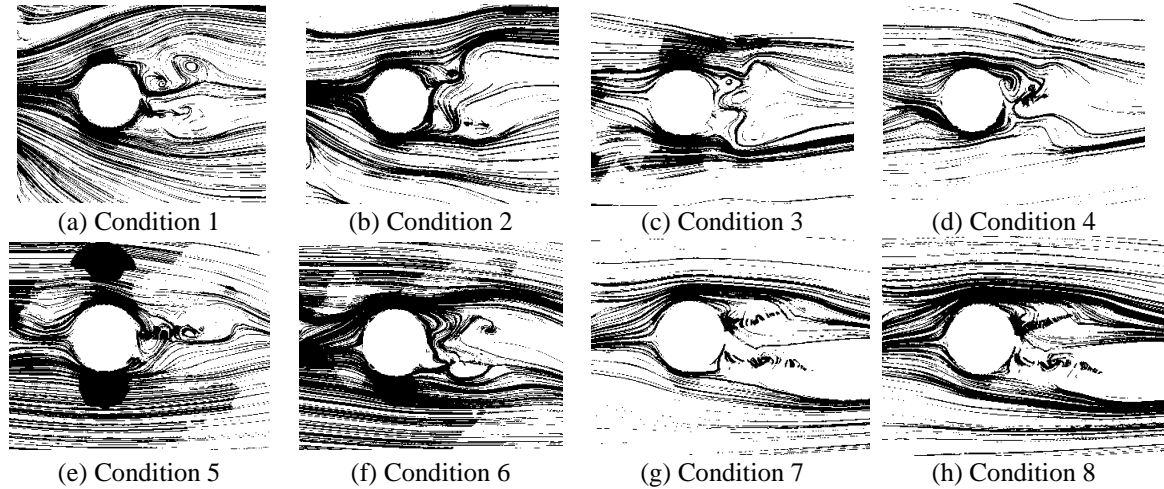


Fig. 15 Velocity streamline of the blades and tower of the wind turbine system at the height with distinct disturbance

Table 4 Lift coefficient and drag coefficient of the tower in different conditions

Location		Condition 1	Condition 2	Condition 3	Condition 4	Condition 5	Condition 6	Condition 7	Condition 8
undisturbed region	C_d	0.514	0.363	0.382	0.323	0.409	0.455	0.622	0.403
	C_l	0.104	0.049	0.052	0.019	-0.035	-0.032	-0.037	-0.107
disturbed region	C_d	0.336	0.336	0.323	0.290	0.167	0.298	0.393	0.345
	C_l	0.030	0.030	-0.149	-0.038	0.309	-0.126	-0.137	-0.082

Fig. 15 shows the velocity streamline of the blades and tower of the wind turbine system at the height with distinct disturbance. It is clear that when the inflow passed through the tower, obvious velocity increment region was formed around the tower. The interacting disturbance effect between the blades and tower at a height close to the top of the tower was significant. Obvious wake vortex was formed at the back of the tower. When the position of the blades and tower was closer, the acceleration of flows around the tower was more significant, the wake vortex region became slender at the back of the tower and the shape of vortex became irregular with the increase in the degree of disturbance between the blades and tower.

4.6 Lift and drag coefficient

According to different relative position of the turbine and tower, the tower can be divided into disturbed region (40 to 85 m) and undisturbed region (0 to 40 m). Table 4 shows lift coefficient and drag coefficient in different regions of the tower. It is evident that lift coefficient was significantly smaller than that of drag coefficient in undisturbed region of the tower. There are some differences in disturbed region under different conditions, due to the obstructive effect of the blades on the

tower, negative pressure distribution was found on the obstructed area on the windward face of the tower, and thus lift coefficient in disturbed region of tower conditions 5 was more than drag coefficient. And lift coefficient increased and drag coefficient reduced when the relative position of the blades and the tower was closer. It is recommended that lift coefficient should be considered in the least favourable condition during the wind resistance design of large scale wind turbine.

5. Conclusions

Numerical analysis was conducted on the effect of different positions of blades on the aerodynamic performance of large scale wind turbine in halt state using LES method. The following conclusions were drawn:

- When the position of the blade was far away from the tower, narrow positive pressure distribution region appeared on the windward face of the tower while negative pressure appeared on the side and leeward faces, and furthermore the negative pressure at the side faces was larger than that on the leeward face. When different extent of obstruction on the tower by the blades occurred, negative pressure distribution region appeared on the obstructed region at the windward face of the tower. With the increase of the degree of obstruction, the negative pressure increased. Due to the obstructive effect of the blades, the negative pressure on the side faces of the tower reduced.
- When the blades completely obstructed the tower, the fluctuating pressure coefficient on the disturbed region of the tower increased significantly. However, the global scale coefficient reduced comparing to other calculating conditions and so was the peak negative pressure at the side faces of the tower.
- Owing to the distribution of negative pressure in the parts of tower windward side which was obscured by blades interference, the maximum peak pressure coefficient was decreased, especially when the blades completely obstructed the tower. The minimum peak wind pressure was appeared on side face of the tower, and the values would be increased when the position was close to the top of the tower. The disturbance of blades also caused the reduction of minimum wind pressure.
- During the process of rotation, obvious apex vortex and blade root vortex appeared in the wake flow field of the blades, and significant trailing edge vortex was produced between the root and apex of the blade. When the relative position of the blades and tower was closer, the wake vortex region at the back of the tower became slender and the shape of vortex became irregular with the increase in the degree of disturbance between the blades and tower.
- Significant flow separation of inflow was found at the location close to the blade root on the leeward face of the blade. The leeward face of the blade mainly consisted of attached flow and small scale attached vortex was formed on the surface of the blade. The flow distributed evenly long the span-wise direction. When the blade completely obstructed the tower, vortex was formed at the centre of the tower by flow around the blade which attached to the flow around the tower and formed large scale vortex at the leeward face of the tower.
- Lift coefficient was significantly smaller than that of drag coefficient in undisturbed region of the tower. Due to the obstructive effect of the blades on the tower, and thus lift coefficient in disturbed region of tower conditions 5 was more than drag coefficient. And lift coefficient increased and drag coefficient reduced when the relative position of the blades and the tower was closer.

Acknowledgments

This work was jointly funded by the National Basic Research Program of China (“973” Program) under Grant No. 2014CB046200, open fund for Jiangsu Key Laboratory of Hi-Tech Research for Wind Turbine Design (ZAA1400206), and China Postdoctoral Science Foundation (2015T80551).

References

- Agarwal, P. and Manuel, L. (2009), “Simulation of offshore wind turbine response for long-term extreme load prediction”, *Eng. Struct.*, **31**(10), 2236-2246.
- Corson, D., Griffith, D.T., Ashwill, T. *et al.* (2012), “Investigating aeroelastic performance of Multi-MegaWatt wind turbine rotors using CFD”, *Proceedings of the 53rd AIAA/ASME/ASCE/AHS/ASC Structures, Structural Dynamics and Materials Conference 20th AIAA/ASME/AHS Adaptive Structures Conference 14th AIAA*.
- Duquette, M.M. and Visser, K.D. (2003), “Numerical implications of solidity and blade number on rotor performance of horizontal-axis wind turbines”, *J. Solar Energy Eng.*, **125**(4), 425-432.
- GB 50009-2012 (2012), Load code for the design of building structures. The Ministry of Structure of the People's Republic of China, Beijing. (in Chinese).
- Greaves, P.R., Dominy, R.G., Ingram, G.L. *et al.* (2012), “Evaluation of dual-axis fatigue testing of large wind turbine blades”, *Proceedings of the Institution of Mechanical Engineers, Part C: Journal of Mechanical Engineering Science*, **226**(7), 1693-1704.
- Griffith, T.D., Carne, T.G. and Paquette, J.A. (2008), “Modal testing for validation of blade models”, *Wind Eng.*, **32**(2), 91-102.
- Guo, T.Q., Lu, Z.L., Tang, D. *et al.* (2013), “A CFD/CSD model for aeroelastic calculations of large-scale wind turbines”, *Sci. China Technol. Sci.*, **56**(1), 205-211.
- Hoogedoorn E., Jacobs G.B. and Beyene A. (2010), “Aero-elastic behavior of a flexible blade for wind turbine application: A 2D computational study”, *Energy*, **35**(2), 778-785.
- Jeong, M.S., Kim, S.W., Lee, I. *et al.* (2013), “The impact of yaw error on aeroelastic characteristics of a horizontal axis wind turbine blade”, *Renew. Energ.*, **60**(5), 256-268.
- Jiménez, Á., Crespo, A. and Migoya, E. (2010), “Application of a LES technique to characterize the wake deflection of a wind turbine in yaw”, *Wind Energy*, **13**(6), 559-572.
- Karimirad, M. and Moan, T. (2011), “Wave-and wind-induced dynamic response of a spar-type offshore wind turbine”, *J. Waterw. Port. C - ASCE*, **138**(1), 9-20.
- Ke, S.T., Ge, Y.J., Wang, T.G. *et al.* (2015), “Wind field simulation and wind-induced responses of large wind turbine tower-blade coupled structure”, *Struct. Des. Tall Spec. Build.*, **24**(8), 571-590.
- Ke, S.T., Wang, T.G., Ge, Y.J. *et al.* (2015), “Aeroelastic responses of ultra large wind turbine tower-blade coupled structures with SSI Effect”, *Adv. Struct. Eng.*, **18**(12), 2075-2087
- Larsen, J.W., Nielsen, S.R.K. and Krenk, S. (2007), “Dynamic stall model for wind turbine airfoils”, *J. Fluid. Struct.*, **23**(7), 959-982.
- Li, X., Lu, Y., Liu, Q. *et al.* (2015), “Experimental study on wind-included interference effects of circular section chimneys”, *Eng. Mech.*, **1**, 159-162. (in Chinese)
- Liu, X., Lu, C., Liang, S. *et al.* (2015), “Influence of the vibration of large-scale wind turbine blade on the aerodynamic load”, *Energy Procedia*, **75**, 873-879.
- Nishimura, H. and Taniike, Y. (2001), “Aerodynamic characteristics of fluctuating forces on a circular cylinder”, *J. Wind Eng. Ind. Aerod.*, **89**(7-8), 713-723.
- Tempel, J.V.D. (2006), Design of support structures for offshore wind turbines. Netherlands: Delft University of Technology.
- Tran, T.T., Kim, D.H. and Nguyen, B.H. (2015), “Aerodynamic interference effect of huge wind turbine blades with periodic surge motions using overset grid-based computational fluid dynamics approach”, *J.*

Solar Energy Eng., **137**(6), 061003.

Wang, H., Li, A., Niu, J., Zong, Z. *et al.* (2013), "Long-term monitoring of wind characteristics at sutong bridge site", *J. Wind Eng. Ind. Aerod.*, **115**(4), 39-47.

CC